

Accepted Manuscript

Design, synthesis, in-silico studies and biological screening of Quinazolinone analogues as potential antibacterial agents against MRSA

Shahnawaz I. Qureshi, Hemchandra K. Chaudhari

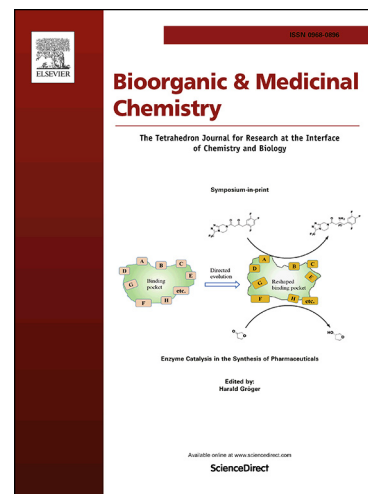
PII: S0968-0896(19)30528-0
DOI: <https://doi.org/10.1016/j.bmc.2019.05.012>
Reference: BMC 14899

To appear in: *Bioorganic & Medicinal Chemistry*

Received Date: 30 March 2019
Revised Date: 6 May 2019
Accepted Date: 7 May 2019

Please cite this article as: Qureshi, S.I., Chaudhari, H.K., Design, synthesis, in-silico studies and biological screening of Quinazolinone analogues as potential antibacterial agents against MRSA, *Bioorganic & Medicinal Chemistry* (2019), doi: <https://doi.org/10.1016/j.bmc.2019.05.012>

This is a PDF file of an unedited manuscript that has been accepted for publication. As a service to our customers we are providing this early version of the manuscript. The manuscript will undergo copyediting, typesetting, and review of the resulting proof before it is published in its final form. Please note that during the production process errors may be discovered which could affect the content, and all legal disclaimers that apply to the journal pertain.



Graphical Abstract

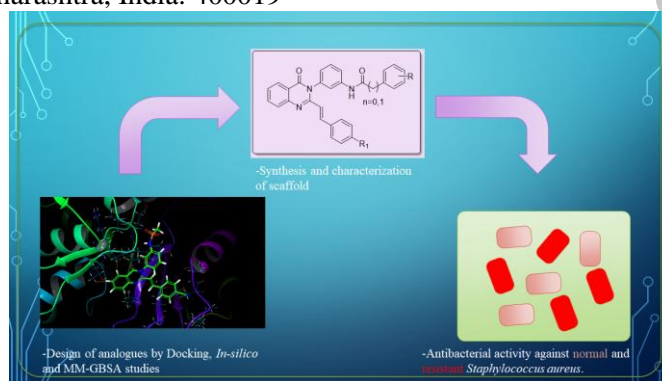
To create your abstract, type over the instructions in the template box below.
Fonts or abstract dimensions should not be changed or altered.

Design, synthesis, in-silico studies and biological screening of Quinazolinone analogues as potential antibacterial agents against MRSA

Shahnawaz I. Qureshi, Hemchandra K. Chaudhari*

Department of Pharmaceutical Sciences and Technology, Institute of Chemical Technology, N. P. Marg, Matunga (E), Mumbai, Maharashtra, India. 400019

Leave this area blank for abstract info.





Design, synthesis, in-silico studies and biological screening of Quinazolinone analogues as potential antibacterial agents against MRSA

Shahnawaz I. Qureshi, Hemchandra K. Chaudhari*

Department of Pharmaceutical Sciences and Technology, Institute of Chemical Technology, N. P. Marg, Matunga (E), Mumbai, Maharashtra, India. 400019

ARTICLE INFO

Article history:

Received

Received in revised form

Accepted

Available online

Keywords:

Penicillin binding protein 2a

Antibacterial

Microbial resistance

Docking

MM-GBSA

ABSTRACT

Type or The emergence of resistance to antibiotic has developed a complicated situation in the treatment of bacterial infections. Considering the antimicrobial resistance phenomenon as one of the greatest challenge of medicinal chemists for search of better anti-bacterial agents, which have potential narrow spectrum activity with low development of resistance potential and low toxicity to host. Cross-linking of peptidoglycan is a key step catalyze by Penicillin binding protein (PBP) to maintain integrity of cell wall in bacterial cell. However, these Penicillin binding protein (PBP) has developed resistance in methicillin-resistant *Staphylococcus aureus* (MRSA) due to acquisition of additional PBP2a. Various Quinazolinone analogues are reported in literature as potential anti-bacterial agents against MRSA. In present study new quinazolinone analogues has been designed, guided by molecular docking, *In-silico* and MM-GBSA study. Newly designed molecules have been synthesized by medicinal chemistry route and their characterization was done by using IR, NMR, & HR-MS techniques. Biological evaluation of synthesized compounds has been done on wild type Gram-negative (*Escherichia coli*), Gram-positive (*Staphylococcus aureus*) and resistant MRSA bacterial strains using Streptomycin, Kanamycin and Linezolid as standard drugs respectively. The in vitro evaluation results have shown that compound **5f** is active with MIC value 15.625 µg/mL against *S. aureus* and with MIC value 31.25 µg/mL against MRSA.

2009 Elsevier Ltd. All rights reserved.

1. Introduction

Antibiotics are among the most frequently prescribed medications today although microbial resistance due to evolutionary pressures and misuses threatens their continued efficacy. Antimicrobial resistance is one of the most serious health threats. Bacterial resistance to antibiotics is growing up day by day in both communities as well as in hospitals. Methicillin-resistant *Staphylococcus aureus* (MRSA) is one of the most widespread and virulent nosocomial pathogens.¹ According to the report of Centers for diseases control and prevention (CDC) of March 2019, it was estimated that nearly 1,19,000 noninvasive Methicillin Resistant *Staphylococcus aureus* (MRSA) infection involving both healthcare and community associated infection, causing more than 20,000 deaths in the year 2017.² The microorganisms mainly involved in the resistance process, were called the ESKAPE pathogens (*Enterococcus faecium*, *Staphylococcus aureus*, *Klebsiella pneumoniae*, *Acinetobacterbaumanii*, *Pseudomonas aeruginosa*, and *enterobacteriaceae*). Among these organisms, Methicillin Resistant *Staphylococcus aureus* (MRSA) alone accounts for most of the death in US than of HIV/AIDS and tuberculosis combined.³ During the past decades, β-lactam antibiotics were the choice of drugs for *S. aureus* infections. However, these agents become ineffective after the emergence of MRSA.⁴ MRSA resistance to β-lactam class of antibiotics developed due

to acquisition of additional penicillin binding protein (PBP), designated PBP2a.⁵

Newer analogs of β-lactam, Cephalosporin antibiotics such as ceftaroline and ceftobiprole are FDA (Food and drug Administration) approved drugs to show anti-MRSA activities. However, they are not orally bioavailable require intravenous infusion after every 8-12 hrs.⁶ The MRSA resistant enzyme has a closed active site regulated by allosteric mechanism hence, β-lactam not able to inhibit MRSA.⁷ Researchers have shown that ceftaroline has an ability to bind non-covalently to the allosteric site at a distance of 60 Å apart from the active site. This binding leads to conformational changes which results in the opening of the active site, and then the another molecule of ceftaroline bind to active site and cause inhibition.⁸ Resistance to this antibiotic has already emerged by disruption of allosteric mechanism.⁹ Other antibiotics has been introduced such as oxazolidinones, linezolid and tedizolid for MRSA strains, however resistance has been already emerged for all these antibiotics.^{10, 11}

There exists an urgent need of novel class of antibiotic for MRSA infections. Researchers has recently reported a new class of antibiotic 4-(3H)-Quinazolinones. The Quinazolinone class of antibacterial is of particular importance; because they do not β-lactam ring but able to inhibit PBP's. This Quinazolinone class of antibacterial has mechanism of action similar to ceftaroline, first they bind non-covalently to allosteric site which then result in

opening of active site and then another molecule of Quinazolinone bind to active site and cause cell wall inhibition.¹²

Literature survey provides various highly active Quinazolinone antibacterial showed several folds higher activity towards the enzyme as compared to standard drugs (Table 1).¹³ An interest was created to study the structural features of these compounds responsible for their high activity against MRSA strains which may be helpful in designing new analogues.

In our paper, we are now reporting a modeling study for design and development of Quinazolinone analogues effective against MRSA strains. These studies can provide useful information for the design of new analogues of Quinazolinone antibacterial with improved activity. Our study includes Structure based design approach docking study using Glide. A reported crystal structure of *S. aureus* PBP2a in complex with Quinazolinone (PDB ID-4CJN) were obtained from protein data bank and performed docking study. Docking procedures were used to identify the correct conformation of ligands in the binding pocket of a protein and to predict the interaction between the ligand and the protein. Docking is one method in which the binding of ligand to a receptor can be explored. Furthermore, Prime MM-GBSA of docked complex has been performed to determine binding free energy. We have also performed Adsorption Distribution, Metabolism and Excretion (ADME) prediction studies. All these studies have been used to design new molecules which then synthesized by appropriate synthetic route and tested against bacterial strains for anti-bacterial activity.

2. Materials and Methods

2.1 Docking studies

Glide module (version 7.1, Schrödinger, LLC, NY) were used to perform the docking studies installed on Redhat Linux workstation.¹⁴ Docking is a process by which the ligand or the inhibitor binds to the receptor site of target protein and they fit together in a 3D space. Docking studies involves the posing, ranking or scoring. Posing involve determination of conformation and orientation of ligands fit at the receptor site. While ranking or scoring involve the estimation of binding free energy when ligand bind to active site which then rank the ligands based on their docking score. Docking study comprises of five steps ligand preparation, protein preparation, receptor grid generation, actual docking procedure and finally viewing the docking results using the pose-viewer.

2.2.1 Ligand & Protein Preparation

As described previously all the ligands for docking studies were prepared by using Lig prep module. Protein preparation was performed by using Protein Preparation Wizard of Maestro software. Crystal structure of *S. aureus* PBP2a in complex with Quinazolinone (PDB ID-4CJN at 1.95 Å resolution) was taken from protein data bank and then the following modification done on protein structure such as add missing hydrogen, assign proper bond orders, treat metal (i.e., delete bonds to metal and adjust the formal charge on metal and neighboring atoms), and to delete water molecules that are more than 5 Å from the heterogeneous groups. The H bonds were optimized using sample orientations. All the polar hydrogen was displayed. Finally, the protein structure was minimized to the default Root Mean Square Deviation (RMSD) value of 0.30. The protein structure was minimized using OPLS 2005 force field. The protein structure thus prepared is ready for docking.

2.1.2. Receptor Grid Generation

Allosteric site: Allosteric site was defined by removing co-crystallized ligand and generating the grid box at the centroid of the workspace ligand as selected in the receptor folder. The grid was generated by applying van der waals radii of 1.0 Å with the partial atomic charge less than 0.25 defaults. The ligands similar in size to the workspace ligand were allowed to dock into the active site. No constraints such as Positional, H-bonding or Hydrophobic were defined.

2.1.3. Active site: No co-crystallized ligand is present at active site. The grid box was generated around the active site for docking by selecting following residues Pro401, Gly402, Ser403, Lys406, Tyr446, Ser461, Ser462, Asp463, Asn464, Ile465, Phe466, Tyr519, Gly520, Gln521, Ser598, Gly599, Thr600, Ala601, Glu602, Leu603, Arg612, Gln613, Ile614, Ala642.¹⁵

2.1.4. Ligand Docking

OPLS 2005 force field was used during docking. The receptor grid generated previously was selected for the docking of ligands prepared using Lig prep. Standard Precision (SP) feature was used to perform flexible docking. The van der waals radii were scaled to 0.80 default and default partial cutoff charge of 0.15 to decrease the penalties for close contacts. No constraints were set to defined ligand-receptor interactions. The structure output form was set to pose viewer file so as to view the output of the resulting docking studies from pose-viewer.

2.1.5. Viewing Docking Results

Pose-Viewer was used to see docking results. The H-bonding and salt bridge interaction between ligands and receptor were visualized using default settings to analyze the binding modes of the ligands to receptor.

No constraints were set to defined ligand-receptor interactions. Computer model score system that encompasses the grid score, proprietary GLIDE score, and the internal energy strain were used to rank the final ligand binding poses. The score function of Glide, or Glide score, was used for binding affinity prediction and ligand ranking.¹⁴

2.2. ADME predictions by QikProp

Almost half of proposed drug fail during the development process, in spite of good efficacy and favorable toxicity profile due to inappropriate pharmacokinetic profile. Therefore, now a days medicinal chemist integrates ADME prediction into drug design and lead optimization strategies. Absorption, Distribution, Metabolism, and Excretion (ADME) prediction software QikProp (version 4.3, Schrödinger, LLC, NY) is a quick, accurate program designed by Professor William L. Jorgensen. QikProp predicts pharmaceutically important properties of organic molecules. In addition to predicting molecular properties, QikProp also provides a range for comparing a particular molecule's properties with those of 95% of known drugs. QikProp also flags 30 types of reactive functional groups that may cause false positives in high-throughput screening (HTS) assays.¹⁶

2.3. MM-GBSA free energy calculations

Molecular Mechanics-Generalized born surface area (MM-GBSA) calculates binding free energies for molecules by combining molecular mechanics calculations and continuum (implicit) solvation models. Molecular mechanics estimates the enthalpy contributions for protein-ligand interaction, whereas implicit solvents models were used to estimate free energies of solute solvent interaction.

The docked poses were minimized using the local optimization feature in Prime and also the ligand strain energies. Energies of

the ligand enzyme complexes were calculated using Prime MM-GBSA technology with all the enzyme residues being held frozen.¹⁷

The binding free energy ΔG_{bind} was estimated by equation below:

$$\Delta G_{\text{bind}} = E_{\text{complex}}(\text{minimized}) - [E_{\text{ligand}}(\text{unbound, minimized}) + E_{\text{receptor}}(\text{unbound, minimized})]$$

Where ΔG_{bind} is the calculated relative free energy that includes both ligand and receptor strain energy. $E_{\text{complex}}(\text{minimized})$ is the MM/GBSA energy of the minimized complex, and $E_{\text{ligand}}(\text{unbound, minimized})$ is the MM/GBSA energy of the ligand after removing it from the complex and allowing it to relax. $E_{\text{receptor}}(\text{unbound, minimized})$ is the MM/GBSA energy of protein after separating it from the ligand.¹⁸

3. Experimental

3.1 Chemicals

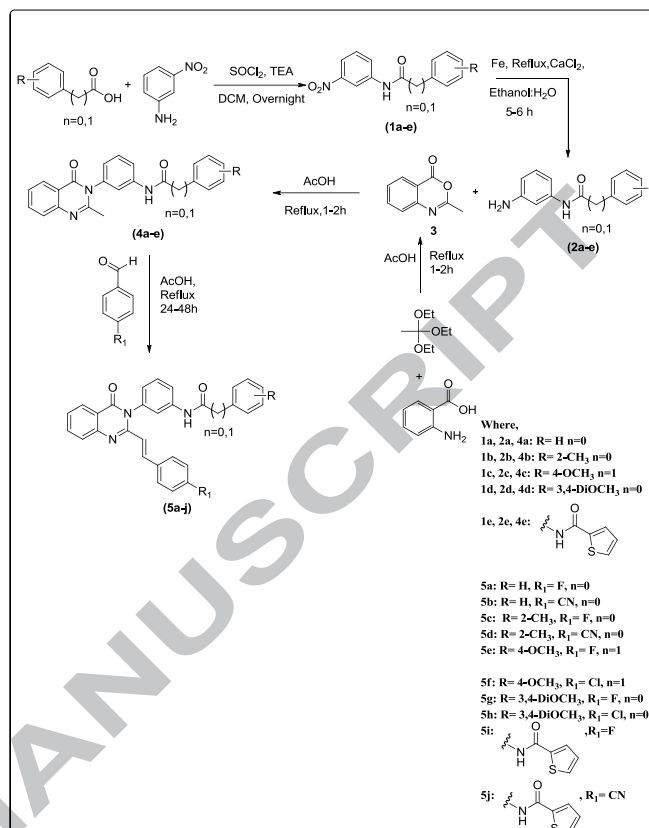
All solvents used were of laboratory grade and were obtained from research gate. Anthranilic acid, triethyl ortho-acetate, 3-nitro aniline, benzoic acid derivatives, benzaldehyde derivatives were commercially available and were obtained from Avra Pvt ltd, and SD fine chemicals.

3.2. Instrumentation

Melting points were determined on Buchi B-545 melting point apparatus. Compounds were routinely checked for purity in Silica Gel Thin Layer Chromatography (TLC) plates and UV lamp was used for visualization of spots. The IR spectra were recorded in KBr pellets on "Perkin Elmer FTIR Spectrophotometer" and "Shimadzu FTIR-Spectrophotometer". ¹H & ¹³C NMR spectra were recorded on 400 MHz NMR spectrometer in CDCl₃ using tetramethylsilane (TMS) as an internal standard. Mass spectra were recorded on Agilent 5975 MSD.

3.3. Antimicrobial Evaluation

Resazurin Microtitre (REMA) Assay, a colorimetric method for determining the ability of drugs/compounds to inhibit viability of bacteria cell is based on reduction of a dye resazurin. Viability of bacterial cells is detected by change in color of the resazurin dye, and the intensity of colour is directly proportional to number of viable bacteria cell present in medium. Resazurin (7-hydroxy-3-oxido-3H-phenoxazine 10-oxide) is a blue dye, it is non-fluorescent in nature, viable bacterial cells irreversibly reduced this dye to pink colored and highly fluorescent end product resorufin. Non-viable cells rapidly lose metabolic capacity and thus not able to generate a fluorescent signal. Resazurin dye is a redox indicator used in cell viability assays for bacteria and mammalian cells etc. Usually it is available commercially as the sodium salt.¹⁹



Scheme 1 Synthesis route for designed Quinazolinone ligands.

3.4. Chemistry

3.4.1 General procedures for preparation of compounds (1a-e)

Carboxylic acid (1.5 eq.) is added to amine (1 eq.) and trimethylamine (TEA) (3 eq.) in dichloromethane (DCM), then 1.5 eq. of thionyl chloride (SOCl₂) is added dropwise at room temperature. The mixture is stirred overnight at room temperature. After completion of reaction as monitored by thin layer chromatography (TLC), the recovery of the reaction product is performed by evaporating the solvent under reduced pressure. The resulting residue is then taken up in ethyl acetate and washed first with 1N HCl and then with 1N NaOH. The organic phase was dried over anhydrous sodium sulphate (Na₂SO₄), and evaporated to dryness under vacuum.²⁰

N-(3-nitrophenyl) benzamide (**1a**). TLC carried out in Hexane: Ethyl acetate (80:20) R_f = 0.37; Molecular formula: C₁₃H₁₀N₂O₃, Nature: light yellow solid, Yield: 60%, M.P: 153-154°C (lit. MP: 152-153°C)²¹, IR: 3360cm⁻¹ (N-H stretch), 1660cm⁻¹ (C=O amide), 1523cm⁻¹ (C-NO₂).

2-methyl-N-(3-nitrophenyl) benzamide (**1b**). TLC carried out in Hexane: Ethyl acetate (80:20) R_f = 0.454; Molecular formula: C₁₄H₁₂N₂O₃, Nature: light yellow solid, Yield: 65%, M.P: 140-14°C, IR: 3287cm⁻¹ (N-H stretch), 2925cm⁻¹ (alkane C-H stretch), 1654cm⁻¹ (C=O amide), 1527cm⁻¹ (C-NO₂).

2-(4-methoxyphenyl)-N-(3-nitrophenyl) acetamide (**1c**). TLC carried out in Hexane: Ethyl acetate (80:20) R_f = 0.5; Molecular formula: C₁₅H₁₄N₂O₃, Nature: yellow solid, Yield: 70%, M.P: 162-163°C, IR: 3243cm⁻¹ (N-H stretch), 1661cm⁻¹ (C=O amide), 1524cm⁻¹ (C-NO₂).

3,4-dimethoxy-N-(3-nitrophenyl) benzamide (**1d**). TLC carried out in Hexane: Ethyl acetate (80:20) R_f = 0.416; Molecular formula: C₁₅H₁₄N₂O₅, Nature: light yellow solid, Yield: 60%,

M.P: 159-160°C, IR: 3322 cm⁻¹ (N-H stretch), 1650 cm⁻¹ (C=O amide), 1510 cm⁻¹ (C-NO₂).

N-(3-nitrophenyl) thiophene-2-carboxamide (**1e**). TLC carried out in Hexane: Ethyl acetate (80:20) R_f = 0.4; Molecular formula: C₁₁H₈N₂O₃S, Nature: light brown solid, Yield: 55%, M.P: 154-155°C, IR: 3379 cm⁻¹ (N-H stretch), 1658 cm⁻¹ (C=O amide), 1527 cm⁻¹ (C-NO₂).

3.4.2 General procedures for preparation of compounds (2a-e):

Dissolve 1eq. of nitro compound in 10mL of Ethanol, 0.5mL of water and then iron powder (3eq.) and Calcium chloride (CaCl₂) (1eq.) were added to the reaction mixture. The resulting reaction mixture was allowed to reflux at 60°C for 4-5 h. Progress of the reaction was monitored by TLC. Spots on TLC plates were visualized under UV lamp or by staining it with 0.2% ninhydrin in ethanol solution and charring after elution. After completion, the reaction mixture was filtered to remove the iron residues; the recovery of the reaction product is performed by evaporating the solvent under reduced pressure. The resulting residue is then taken up in ethyl acetate. The organic extracts were washed with H₂O (3 × 10 mL), brine (2 × 10 mL), and dried over Na₂SO₄, the organic phase was evaporated. Purification of the compound has been performed by Silica column chromatography using Hexane: Ethyl acetate (80:20) as eluting solvent.²²

N-(3-aminophenyl) benzamide (**2a**). TLC carried out in Hexane: Ethyl acetate (70:30) R_f = 0.136; Molecular formula: C₁₃H₁₂N₂O, Nature: light brown solid, Yield: 80%, M.P: 119-120°C (lit. MP: 124°C)²³, IR: 3435cm⁻¹ and 3346cm⁻¹ (NH₂ stretch), 1654cm⁻¹ (C=O amide).

N-(3-aminophenyl)-2-methyl benzamide (**2b**). TLC carried out in Hexane: Ethyl acetate (70:30) R_f = 0.16; Molecular formula: C₁₄H₁₄N₂O, Nature: light brown solid, Yield: 80%, M.P: 135-136°C, IR: 3435cm⁻¹ and 3350cm⁻¹ (NH₂ stretch), 2925cm⁻¹ (alkane C-H stretch), 1644cm⁻¹ (C=O amide).

N-(3-aminophenyl)-2-(4-methoxyphenyl) acetamide (**2c**). TLC carried out in Hexane: Ethyl acetate (70:30) R_f = 0.12; Molecular formula: C₁₅H₁₆N₂O₂, Nature: light brown solid, Yield: 75%, M.P: 122-123°C, IR: 3435cm⁻¹ and 3346cm⁻¹ (NH₂ stretch), 2926cm⁻¹ (alkane C-H stretch), 1651cm⁻¹ (C=O amide).

N-(3-aminophenyl)-3,4-dimethoxybenzamide (**2d**). TLC carried out in Hexane: Ethyl acetate (70:30) R_f = 0.096; Molecular formula: C₁₅H₁₆N₂O₃, Nature: brown solid, Yield: 70%, M.P: 131-132°C, IR: 3371 cm⁻¹ and 3289 cm⁻¹ (NH₂ stretch), 2841 cm⁻¹ (alkane C-H stretch), 1649cm⁻¹ (C=O amide).

N-(3-aminophenyl) thiophene-2-carboxamide (**2e**). TLC carried out in Hexane: Ethyl acetate (70:30) R_f = 0.12; Molecular formula: C₁₁H₁₀N₂OS, Nature: brown solid, Yield: 70%, M.P: 132°C, IR: 32296 cm⁻¹ and 3194cm⁻¹ (NH₂ stretch), 1662cm⁻¹ (C=O amide).

3.4.3. General procedures for preparation of compound (3): A stirred mixture of anthranilic acid (1eq.) and triethyl ortho-acetate (2eq.) was heated under reflux for 15-20 min. Progress of the reaction was monitored by TLC. After completion of reaction (as monitored by TLC), the reaction mixture was allowed to cooled to 0 °C and the precipitate thus obtained was filtered off and recrystallized from hexane to give white to yellow needles like crystals.²⁴

2-methyl-4H-benzo[d][1,3]oxazin-4-one (**3**). TLC carried out in Hexane: Ethyl acetate (90:10) R_f = 0.481; Molecular formula: C₉H₇NO₂, Nature: light brown solid, Yield: 75%, M.P: 80°C, IR: 2970cm⁻¹ (alkane C-H stretch), 1738cm⁻¹ (lactone C=O),

3.4.4. General procedures for preparation of compounds (4a-e): Compound (**1a-e**) (1eq.) and compound (**2a-e**) (1eq.) were suspended in 5 mL of glacial acetic acid. The suspension dissolved completely upon heating. The reaction was refluxed for 15-30min. After completion of reaction (as monitored by TLC), reaction mixture was allowed to cooled, and then 10 mL of water was added. The resulting precipitate was then filtered and was washed with water, cold ethanol, and hexanes to give the product.²⁵

N-(3-(2-methyl-4-oxoquinazolin-3(4H)-yl)phenyl) benzamide (**4a**): TLC carried out in Hexane: Ethyl acetate (60:40) R_f = 0.13; cream color solid (70%); M.P: 248-249°C; IR: 3290cm⁻¹ (N-H stretch), 1658cm⁻¹ (C=O amide); HRMS: m/z calcd for C₂₂H₁₇N₃O₂: 355.39 [M+H]⁺; found: 356.1565.

2-methyl-N-(3-(2-methyl-4-oxoquinazolin-3(4H)-yl)phenyl) benzamide (**4b**). TLC carried out in Hexane: Ethyl acetate (60:40) R_f = 0.192; cream color solid (70%); M.P: 239-240°C; ¹H NMR (400 MHz, CDCl₃) δ 8.43 (s, 1H), 8.15 (d, J = 8.0 Hz, 1H), 7.81 – 7.72 (m, 2H), 7.65 (d, J = 8.1 Hz, 1H), 7.50 (d, J = 8.0 Hz, 1H), 7.44 (t, J = 7.2 Hz, 2H), 7.38 (t, J = 8.0 Hz, 1H), 7.21 (d, J = 7.4 Hz, 1H), 7.15 (d, J = 7.4 Hz, 1H), 7.10 (t, J = 7.4 Hz, 1H), 6.81 (d, J = 7.7 Hz, 1H), 2.47 (s, 3H), 2.27 (s, 3H); ¹³C NMR (101 MHz, CDCl₃) δ 168.24 (s), 162.42 (s), 154.09 (s), 147.44 (s), 140.09 (s), 137.88 (s), 136.44 (s), 135.82 (s), 134.72 (s), 131.09 (s), 130.21 (s), 130.17 (s), 126.93 (s), 126.88 (s), 126.79 (s), 126.63 (s), 125.60 (s), 123.13 (s), 120.52 (s), 120.45 (s), 119.53 (s), 30.93 (s), 24.32 (s); IR: 3308 (N-H stretch), 2970 (alkane C-H stretch), 1661 (C=O amide) cm⁻¹; HRMS: m/z calcd for C₂₃H₁₉N₃O₂: 369.42 [M+H]⁺; found: 370.1740.

2-(4-methoxyphenyl)-N-(3-(2-methyl-4-oxoquinazolin-3(4H)-yl)phenyl) acetamide (**4c**). TLC carried out in Hexane: Ethyl acetate (50:50) R_f = 0.088; Nature: cream color solid (70%); M.P: 202-203°C; IR: 3278cm⁻¹ (N-H stretch), 2933 cm⁻¹ (C-H stretch, alkane) 1656cm⁻¹ (C=O amide); HRMS: m/z calcd for C₂₄H₂₁N₃O₃: 399.16 [M+H]⁺; found: 399.8000.

3,4-dimethoxy-N-(3-(2-methyl-4-oxoquinazolin-3(4H)-yl)phenyl) benzamide (**4d**). TLC carried out in Hexane: Ethyl acetate (50:50) R_f = 0.115; Nature: cream color solid (70%); M.P: 246-247°C; IR: 3268cm⁻¹ (N-H stretch), 1655 cm⁻¹ (C=O amide); HRMS: m/z calcd for C₂₄H₂₁N₃O₄: 415.15 [M+H]⁺; found: 415.8000.

N-(3-(2-methyl-4-oxoquinazolin-3(4H)-yl)phenyl)thiophene-2-carboxamide (**4e**). TLC carried out in Hexane: Ethyl acetate (60:40) R_f = 0.157; Nature: cream color solid (70%); M.P: 279-280°C; IR: 3340 cm⁻¹ (N-H stretch), 3078 cm⁻¹ (alkane C-H stretch), 1666 cm⁻¹ (C=O amide); HRMS: m/z calcd for C₂₀H₁₅N₃O₂S: 360.12 [M+H]⁺; found: 361.9000.

3.4.5. General procedures for preparation of compounds (5a-j): Compound (**4a-e**) (1eq.) was suspended in 5 mL of glacial acetic acid and dissolved upon heating, to which substituted benzaldehyde (1eq.) was added. The reaction was then refluxed for 24-48 h. Progress of the reaction monitored by TLC. After completion of reaction, 10 mL of water was added to the cooled reaction mixture. The resulting precipitate was filtered and washed with water followed by cold ethanol and hexanes to give the product. Purification of the products has been performed by Silica column chromatography using Hexane: Ethyl acetate (70:30) as eluting solvent.²⁶

(E)-N-(3-(2-(4-fluorostyryl)-4-oxoquinazolin-3(4H)-yl)phenyl)benzamide (**5a**). TLC carried out in Hexane: Ethyl acetate (60:40) R_f = 0.260; Nature: yellow solid, Yield: 60%, M.P: 267-268°C, IR: 3345cm⁻¹ (N-H stretch), 1664cm⁻¹ (C=O amide), 1602cm⁻¹ (alkene C=C stretch); HRMS: m/z calcd for C₂₉H₂₀FN₃O₂: 461.49 [M+H]⁺; found: 462.1791.

(E)-N-(3-(2-(4-cyanostyryl)-4-oxoquinazolin-3(4H)-yl)phenyl)benzamide (**5b**). TLC carried out in Hexane: Ethyl acetate (60:40) $R_f = 0.32$; Nature: light yellow solid, Yield: 50%, M.P: 290°C, $^1\text{H NMR}$ (400 MHz, CDCl_3) δ 9.48 (s, 1H), 8.21 (d, $J = 8.6$ Hz, 1H), 7.87 (d, $J = 14.1$ Hz, 1H), 7.85 (d, $J = 5.3$ Hz, 4H), 7.73 (d, $J = 5.1$ Hz, 2H), 7.50 (d, $J = 7.7$ Hz, 2H), 7.43 (d, $J = 7.9$ Hz, 3H), 7.36 (dd, $J = 10.3, 7.2$ Hz, 4H), 6.91 (d, $J = 7.8$ Hz, 1H), 6.52 (d, $J = 15.5$ Hz, 1H); IR: 3330 cm^{-1} (N-H stretch), 2223 cm^{-1} (CN stretch), 1658 cm^{-1} (C=O amide), 1604 cm^{-1} (alkene C=C stretch), HRMS: m/z calcd for $\text{C}_{30}\text{H}_{20}\text{N}_4\text{O}_2$: 468.25 $[\text{M}+\text{H}]^+$; found: 469.2000.

(E)-N-(3-(2-(4-fluorostyryl)-4-oxoquinazolin-3(4H)-yl)phenyl)-2-methyl benzamide (**5c**). TLC carried out in Hexane: Ethyl acetate (60:40) $R_f = 0.348$; cream color solid, Yield: 60%, M.P: 214-215°C, $^1\text{H NMR}$ (400 MHz, CDCl_3) δ 8.22 (d, $J = 7.9$ Hz, 2H), 7.93 (d, $J = 15.5$ Hz, 1H), 7.79 (dd, $J = 16.8, 7.6$ Hz, 3H), 7.67 (d, $J = 11.3$ Hz, 1H), 7.45 (d, $J = 7.6$ Hz, 4H), 7.38 – 7.29 (m, 2H), 7.19 (d, $J = 6.4$ Hz, 1H), 7.13 (s, 1H), 6.99 (t, $J = 8.5$ Hz, 2H), 6.86 (s, 1H), 6.37 (d, $J = 15.6$ Hz, 1H), 2.49 (s, 3H); $^{13}\text{C NMR}$ (101 MHz, CDCl_3) δ 168.15 (s), 164.71 (s), 162.35 (s), 162.21 (s), 151.33 (s), 147.70 (s), 138.89 (s), 136.65 (s), 135.73 (s), 134.76 (s), 131.48 (s), 131.45 (s), 131.20 (s), 130.34 (s), 129.75 (s), 129.67 (s), 127.34 (s), 127.08 (s), 126.83 (s), 126.65 (s), 125.65 (s), 123.94 (s), 123.90 (s), 120.62 (s), 120.58 (s), 119.90 (s), 119.40 (s), 115.99 (s), 115.78 (s), 30.93 (s); IR: 3288 cm^{-1} (N-H stretch), 2927 cm^{-1} (alkene C-H stretch), 1656 cm^{-1} (C=O amide), 1601 cm^{-1} (alkene C=C stretch), HRMS: m/z calcd for $\text{C}_{30}\text{H}_{22}\text{FN}_3\text{O}_2$: 475.0025 $[\text{M}+\text{H}]^+$; found: 476.1943.

(E)-N-(3-(2-(4-cyanostyryl)-4-oxoquinazolin-3(4H)-yl)phenyl)-2-methyl benzamide (**5d**). TLC carried out in Hexane: Ethyl acetate (60:40) $R_f = 0.442$; light yellow, Yield: 65%, M.P: 245-246°C, $^1\text{H NMR}$ (400 MHz, CDCl_3) δ 8.23 (d, $J = 7.4$ Hz, 1H), 8.17 (s, 1H), 7.94 (d, $J = 15.5$ Hz, 1H), 7.77 (d, $J = 7.8$ Hz, 3H), 7.69 (d, $J = 7.4$ Hz, 1H), 7.57 (d, $J = 8.2$ Hz, 2H), 7.53 – 7.37 (m, 5H), 7.27 (s, 1H), 7.19 (d, $J = 7.1$ Hz, 1H), 7.14 (t, $J = 7.1$ Hz, 1H), 6.90 (d, $J = 6.9$ Hz, 1H), 6.56 (d, $J = 15.5$ Hz, 1H), 2.48 (s, 3H); IR: 3255 cm^{-1} (N-H stretch), 2228 cm^{-1} (CN stretch), 1665 cm^{-1} (C=O amide), 1603 cm^{-1} (alkene C=C stretch), HRMS: m/z calcd for $\text{C}_{31}\text{H}_{22}\text{N}_4\text{O}_2$: 482.9018 $[\text{M}+\text{H}]^+$; found: 482.9000.

(E)-N-(3-(2-(4-fluorostyryl)-4-oxoquinazolin-3(4H)-yl)phenyl)-2-(4-methoxyphenyl)acetamide (**5e**). TLC carried out in Hexane: Ethyl acetate (50:50) $R_f = 0.25$; brownish yellow solid (60%); M.P: 236-23°C, $^1\text{H NMR}$ (400 MHz, CDCl_3) δ 8.29 (d, $J = 7.8$ Hz, 1H), 8.20 (s, 1H), 7.90 (d, $J = 15.5$ Hz, 1H), 7.78 (d, $J = 5.2$ Hz, 2H), 7.69 (d, $J = 8.8$ Hz, 1H), 7.56 – 7.44 (m, 1H), 7.44 – 7.34 (m, 2H), 7.29 – 7.16 (m, 6H), 6.91 (d, $J = 7.3$ Hz, 1H), 6.85 (d, $J = 8.5$ Hz, 2H), 6.35 (d, $J = 15.5$ Hz, 1H), 3.76 (s, 3H), 3.51 (s, 2H); $^{13}\text{C NMR}$ (101 MHz, CDCl_3) δ 169.82 (s), 162.70 (s), 151.18 (s), 147.80 (s), 140.16 (s), 138.88 (s), 136.97 (s), 135.53 (s), 134.88 (s), 133.62 (s), 130.49 (s), 130.33 (s), 129.04 (s), 129.01 (s), 128.75 (s), 127.50 (s), 127.05 (s), 126.81 (s), 126.37 (s), 123.37 (s), 123.35 (s), 120.74 (s), 120.62 (s), 120.54 (s), 120.02 (s), 119.58 (s), 119.21 (s), 114.35 (s), 114.32 (s), 55.24 (s), 43.62 (s); IR: 3276 cm^{-1} (N-H stretch), 1646 cm^{-1} (C=O amide), 1689 cm^{-1} (alkene C=C stretch); HRMS: m/z calcd for $\text{C}_{31}\text{H}_{24}\text{FN}_3\text{O}_3$: 505.8025 $[\text{M}+\text{H}]^+$; found: 505.8000.

(E)-N-(3-(2-(4-chlorostyryl)-4-oxoquinazolin-3(4H)-yl)phenyl)-2-(4-methoxyphenyl)acetamide (**5f**). TLC carried out in Hexane: Ethyl acetate (50:50) $R_f = 0.36$; light yellow solid (45%); M.P: 243-244°C, $^1\text{H NMR}$ (400 MHz, CDCl_3) δ : 8.34 (s, 1H), 8.29 (d, $J = 8.1$ Hz, 1H), 7.92 (d, $J = 15.4$ Hz, 1H), 7.78 (d, $J = 8$ Hz, 2H), 7.70 (d, $J = 7.5$ Hz, 1H), 7.54 – 7.43 (m, $J = 4$ Hz, 1H), 7.38 (d, $J = 8$ Hz, 2H), 7.28 (dd, $J = 8.4, 5.3$ Hz, 2H), 7.21 (d, $J = 8.4$ Hz, 2H), 6.96 (t, $J = 8.5$ Hz, 2H), 6.90 (d, $J = 7.3$ Hz, 1H), 6.84 (d, $J = 8.5$ Hz, 2H), 6.30 (d, $J = 15.5$ Hz, 1H), 3.75 (s, 3H), 3.49 (s,

2H); $^{13}\text{C NMR}$ (101 MHz, CDCl_3) δ : 169.86, 162.81, 158.85, 153.09, 151.33, 147.87, 140.27, 139.06, 136.99, 134.87, 131.39, 131.35, 130.46, 130.31, 129.76, 129.67, 127.47, 127.04, 126.71, 126.46, 123.29, 120.77, 120.56, 119.59, 119.22, 119.18, 115.98, 115.76, 114.29, 55.23, 43.57; IR: 3276 cm^{-1} (N-H stretch), 3070 cm^{-1} (alkene C=C-H stretch), 2929 cm^{-1} (alkane C-H stretch), 1656 cm^{-1} (C=O amide), 1601 cm^{-1} (alkene C=C stretch), 808 cm^{-1} (C-Cl stretch); HRMS: m/z calcd for $\text{C}_{31}\text{H}_{24}\text{ClN}_3\text{O}_3$: found: $[\text{M}+\text{H}]^+$: 521.7, $[\text{M}+\text{H}]^{++}$: 523.7.

(E)-N-(3-(2-(4-fluorostyryl)-4-oxoquinazolin-3(4H)-yl)phenyl)-3,4-dimethoxybenzamide (**5g**). TLC carried out in Hexane: Ethyl acetate (50:50) $R_f = 0.260$; cream color solid (50%); M.P: 239-240°C, $^1\text{H NMR}$ (400 MHz, CDCl_3) δ 8.64 (s, 1H), 8.29 (d, $J = 7.5$ Hz, 1H), 7.92 (d, $J = 11.8$ Hz, 1H), 7.89 (s, 1H), 7.78 (d, $J = 5.0$ Hz, 2H), 7.62 (s, 1H), 7.52 – 7.40 (m, 3H), 7.37 (t, $J = 8.0$ Hz, 1H), 7.29 (dd, $J = 8.4, 5.4$ Hz, 2H), 6.96 (t, $J = 8.5$ Hz, 2H), 6.75 (dd, $J = 16.2, 7.9$ Hz, 2H), 6.33 (d, $J = 15.5$ Hz, 1H), 3.85 (s, 3H), 3.85 (s, 3H); IR: 3465 cm^{-1} (N-H stretch), 3083 cm^{-1} (alkene C=C-H stretch), 2938 cm^{-1} (alkane C-H stretch), 1676 cm^{-1} (C=O amide), 1601 cm^{-1} (alkene C=C stretch), HRMS: m/z calcd for $\text{C}_{31}\text{H}_{24}\text{FN}_3\text{O}_4$: 521.22 $[\text{M}+\text{H}]^+$; found: 522.3000.

(E)-N-(3-(2-(4-chlorostyryl)-4-oxoquinazolin-3(4H)-yl)phenyl)-3,4-dimethoxybenzamide (**5h**). TLC carried out in Hexane: Ethyl acetate (50:50) $R_f = 0.291$; cream color solid, (45%); M.P: 251-252°C, IR: 3346 cm^{-1} (N-H stretch), 2934 cm^{-1} (alkane C-H stretch), 1661 cm^{-1} (C=O amide), 1603 cm^{-1} (alkene C=C stretch), HRMS: m/z calcd for $\text{C}_{31}\text{H}_{24}\text{ClN}_3\text{O}_4$: 537.15 $[\text{M}+\text{H}]^+$; found: $[\text{M}+\text{H}]^+$: 537.8, $[\text{M}+\text{H}]^{++}$: 539.8.

(E)-N-(3-(2-(4-fluorostyryl)-4-oxoquinazolin-3(4H)-yl)phenyl)thiophene-2-carboxamide (**5i**). TLC carried out in Hexane: Ethyl acetate (50:50) $R_f = 0.368$; Cream color solid (60%); M.P: above 295°C, IR: 3325 cm^{-1} (N-H stretch), 3078 cm^{-1} (alkene C=C-H stretch) 1658 cm^{-1} (C=O amide), 1604 cm^{-1} (alkene C=C stretch), HRMS: m/z calcd for $\text{C}_{27}\text{H}_{18}\text{FN}_3\text{O}_2\text{S}$: 467.11 $[\text{M}+\text{H}]^+$; found: 468.0000.

(E)-N-(3-(2-(4-cyanostyryl)-4-oxoquinazolin-3(4H)-yl)phenyl)thiophene-2-carboxamide (**5j**). TLC carried out in Hexane: Ethyl acetate (50:50) $R_f = 0.259$; Light brown (55%); M.P: above 295°C, IR: 3340 cm^{-1} (N-H stretch), 3066 cm^{-1} (alkene C=C-H stretch) 2222 cm^{-1} (CN stretch), 1666 cm^{-1} (C=O amide); HRMS: m/z calcd for $\text{C}_{28}\text{H}_{18}\text{N}_4\text{O}_2$: 474.12 $[\text{M}+\text{H}]^+$; found: 474.8000.

3.5. Testing of Antimicrobial activity

The MIC of synthesized molecules was determined by micro broth dilution method i.e. Resazurin microtitre assay method (REMA). The following steps were carried out:

Preparation of Nutrient broth (200 ml):

Material required:

Nutrient broth.....3.25 g

Distilled water.....250 ml

Method

The nutrient broth was dissolved in 250 ml of water. The media was then sterilized by moist heat sterilization method using autoclave. The freshly prepared and sterilized media was used for evaluation.

Preparation of bacterial cell culture: The strains of *S. aureus* (wild type), *E. coli* (wild type) was obtained from institute itself, while the strain of Methicillin Resistant *Staphylococcus aureus* (MRSA) (ATCC 33592) was obtained from National facility of

biopharmaceuticals, G N Khalsa College. The cultures of bacterial strains were prepared individually by inoculating in nutrient broth and kept in incubator for 24h at temperature 37 °C, OD₅₈₀ adjusted to 0.1 (approx. 10⁷ cells/mL).

Preparation of drug and test compound stock solution: Stock solution (5mg/ml) of the test compounds and standard drug were prepared in DMSO in 2 mL of Eppendorf tube. In case of Wild type strains Streptomycin and kanamycin is used as standard drugs, while linezolid was used as standard drug in MRSA strains. Dilution of stock solution: 100µL of stock solution of test compound was taken into an Eppendorf tube and volume was made up to 1mL with nutrient broth. From this 100 µL of solution was serially diluted into each well of 96 microtitre plate which previously contained 100µL of nutrient broth. Preparation of 0.02% Resazurin solution: 20mg of Resazurin solution was dissolved into 100mL of sterile water.

3.6. Assay protocol

100µL of nutrient broth was added into each well of the microtitre plate.

100µL test compound was added into the 1st well of a particular concentration and serially diluted (two-fold dilution) till 5th well i.e. four dilutions. 100µL of homogenized bacterial cell culture suspension (10⁵ cells per well) was added to all the wells (well with or without drug). After this, the plate was labelled and it was incubated at 37°C for 20-24 h in incubator. After 24 h, 30µL of 0.02 % Resazurin solution was added, plate was observed after 30 min. and MIC was determined by visual inspection of color change from blue (inhibition) to pink (growth).²⁷

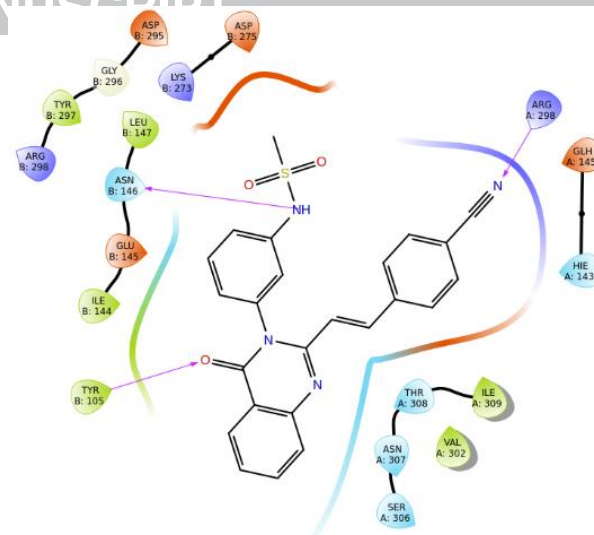


Figure 2. 2D Interaction between most active reported molecule **A** and amino acid present in Penicillin binding protein **2a** (4CJN) at allosteric site.

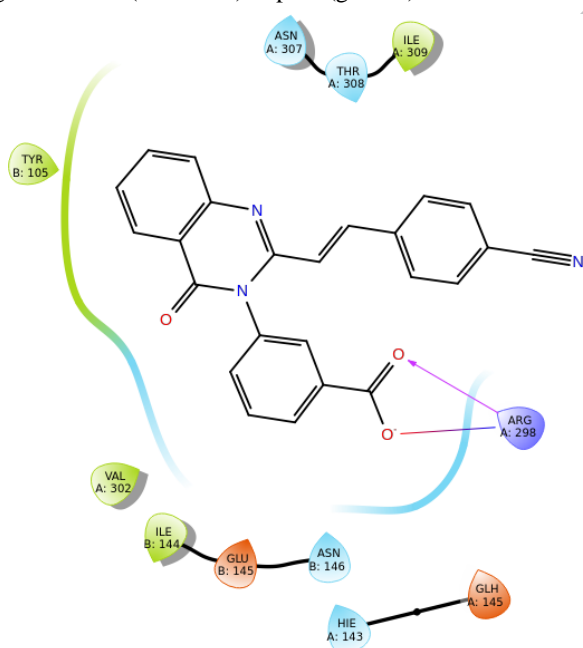


Figure 1. 2D Interaction between native ligand and amino acid present in Penicillin binding protein **2a** (4CJN) at allosteric site

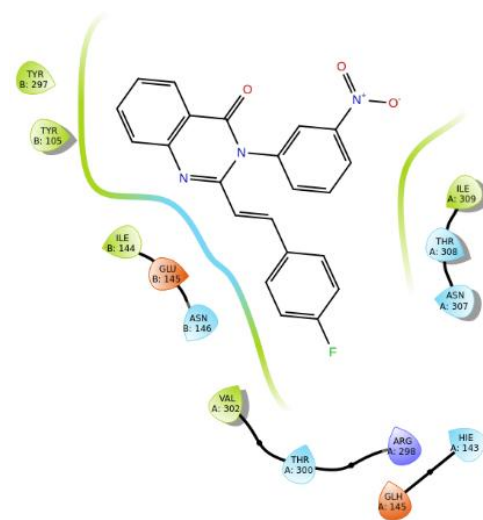


Figure 3. 2D Interaction between least active reported molecule **B** and amino acid present in Penicillin binding protein **2a** (4CJN) at allosteric site.

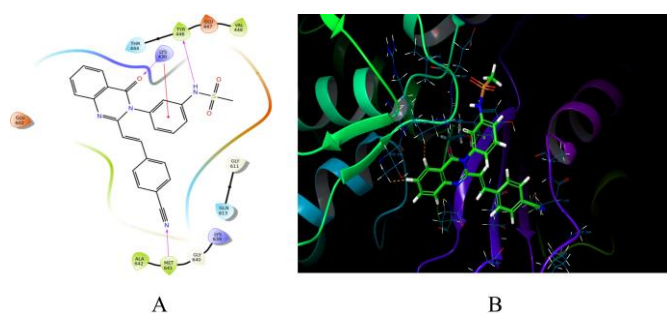


Figure 4. A) 2D and B) 3D Interaction between most active reported molecule **A** and amino acid present in Penicillin binding protein 2a (4CJN) at active site.

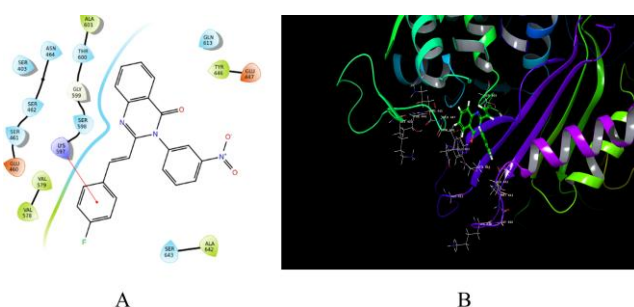


Figure 5. A) 2D and B) 3D Interaction between least active reported molecule **B** and amino acid present in Penicillin binding protein 2a (4CJN) at active site.

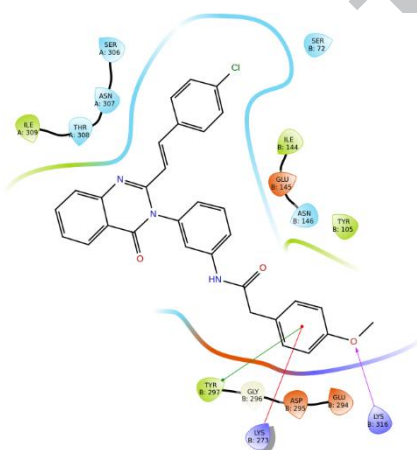


Figure 6. 2D Interaction between most docked ligand **8** and amino acid present in target protein (4CJN) at allosteric site.

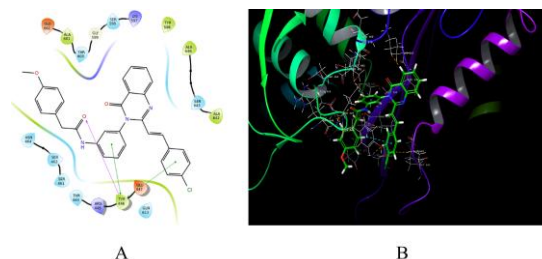


Figure 7. A) 2D and B) 3D Interaction between most docked ligand **8** and amino acid present in target protein (4CJN) at active site.

4. Results and Discussion

4.1 Molecular Docking

4.1.1 Allosteric site

All molecules were docked using 4CJN target protein. Validation of the docking was performed by removing the co-crystallized ligand (Native ligand) from the allosteric site and then re-docked to the same site, and the RMSD was found to be 0.014 Å (less than 2Å). To further validate the docking results, we have incorporated two marketed active drug molecule such as ceftaroline (active moiety of prodrug ceftarolinefosamil) and ceftobiprole (active moiety of prodrug ceftobiprole medocaril) in our docking study.⁸ Result of docking studies in form of docking score is shown in Table 1.

The results showed that the marketed drug ceftaroline and ceftobiprole has docking score of -5.558Kcal/mol and -4.64 Kcal/mol. The result indicates that most active reported molecule **A** has the little lower binding affinity towards PBP2a as compared to marketed drugs with docking score of -4.579 Kcal/mol. However, most active reported molecule **A** has higher binding affinity than a native ligand (reported molecule). The docking score of native ligand was found to be -3.581 kcal/mol. Also, we observed that least active reported molecule **B** from data set has lowest binding affinity towards PBP2a with docking score of -1.199 Kcal/mol.

The binding pose of native ligand molecule (re-docked pose) is shown in Figure 1. Several favorable interactions between ligand and enzyme were observed; ligand shows two hydrogen bonding interaction (pink dotted line) between oxygen of carboxylic acid with ARG298.

The binding pose of most active reported molecule **A** is shown in Figure 2. Several favorable interactions between ligand and enzyme were observed; ligand shows three hydrogen bonding interaction (pink dotted line) with receptor include nitrogen of mesyl group with ASN146; Nitrogen Cyano grp with ARG293; oxygen of Quinazolinone ring with TYR105.

The binding pose of least active reported molecule **B** is shown in Figure 3. No favorable interactions between ligand and enzyme were observed. This docking interaction with least active molecule **B** indicate that electron withdrawing group might be unfavorable. Therefore, the least active reported molecule **B** is showing least docking score.

4.1.2 Active site

Similarly, to validate the docking results, we have included two marketed active drug molecule such as ceftaroline and ceftobiprole in our docking study. Result of docking studies in form of docking score is shown in Table 1.

The results showed that the marketed drug ceftaroline and ceftobiprole has docking score of -5.334Kcal/mol and -5.291 Kcal/mol at active site. The result indicates that most active reported molecule **A** has the little lower binding affinity towards PBP2a as compared to marketed drugs with docking score of -4.834 Kcal/mol. However, most active reported molecule **A** has little higher binding affinity than a native ligand. The docking score of native ligand was found to be -4.795 kcal/mol. Also, we observed that least active reported molecule **B** from data set has lowest binding affinity towards PBP2a with docking score of -1.603 Kcal/mol.

The binding pose of most active reported molecule **A** at active site in 2D and 3D image is shown in Figure 4; Several favorable interactions between ligand and enzyme was observed in 2D interaction image, H-bond interaction (pink dotted line) between nitrogen of mesyl group and TYR446, oxygen of quinazolinone with LYS430 and nitrogen of cyano group with MET641. It also shows π -cation interaction (red line) with LYS430. 3D interaction image shows weak H-bond interaction (orange dotted line) with various residues but no interaction with SER403 residue which is required for acylation in case of β -lactam antibiotics. Hence it indicates that non-covalent interactions at active site may be important for activity.

The binding pose of least active reported molecule **B** at active in 2D and 3D interaction image is shown in Figure 5; 2D interaction image shows only one π -cation interaction (red line) with LYS597. 3D interaction image shows weak H-bond interaction (orange dotted line). Here also no interaction with SER403 residue. Similar to allosteric site, the least active reported molecule **B** is not showing much interaction with the amino acid residues. These may conclude that the reasons for low activity of least active reported molecule might be due to less or no interaction with residue at allosteric and active site.

The docking study concludes that quinazolinone molecule is not showing any interaction with SER403 at active site, which indicate that the anti-bacterial activity of molecules may be due to non-covalent interactions. The most active reported molecule **A** shows several favorable interactions with substitution present at 3 position of quinazolinone at both allosteric and active site, may be this position is important for modification to further improve in activity. Docking study can be used to design new more potent analogues.

4.1.3 In-silico pharmacokinetic prediction

QikProp software gives predicted information about molecular weight, partition coefficient (logPo/w), stars, % oral absorption values and Lipinski's properties (Rule of Five) and apparent Caco-2 cell permeability (QPPCaco) in nm/sec. To validate the result of In-silico studies, we have incorporated two marketed prodrugs such as ceftaroline fosamil and ceftobiprole medocaril in our ADMET prediction study. We were studied 77 compounds from that most active and least active reported molecules **B** along with the prodrug ceftaroline fosamil and ceftobiprole medocaril are mentioned in Table 2.

For the 77 reported molecules, the partition coefficient (logPo/w) was found to be in range between 2.3 to 5.1 resemble with drugs ceftaroline fosamil and ceftobiprole medocaril for the estimation of absorption and distribution of drug within the body.

Caco-2 cell permeability (QPPCaco), a key factor to determine drug metabolism and its access to biological membrane ranged in between 0.568 to 1151.21nm/sec, from which most active molecule shows an absorption value of 853.02 nm/sec, more than the active drugs ceftaroline fosamil and

ceftobiprole medocaril. Overall, the percentage human oral absorption for 77 reported molecules ranged from 38.37% to 100%.

All these pharmacokinetic parameters were found to be within acceptable range defined for human use see in Table 2, thereby indicating their potential as drug-like molecule.

4.1.4 Prime MM-GBSA calculations

The top ranked molecules were further subjected to Prime MM-GBSA calculations (Table 1). At allosteric site, the most active reported molecule **A** was found to have binding free energy (dG bind) of -47.41kcal/mol, slightly lower than drug ceftaroline which has highest binding free energy (dG bind) of -50.36 kcal/mol, while dG bind of drug ceftobiprole was found to be -42.13kcal/mol slightly lower than most active reported molecule **A**. Whereas native ligand has lower binding free energy compare to most active reported molecule **A** of -38.35kcal/mol and least active reported molecule **B** has weaker binding free energy of -22.42 kcal/mol. Similarly, at active site most active reported molecule **A** was found to have binding free energy (dG bind) of -43.43kcal/mol, slightly lower than drugs ceftaroline and ceftobiprole which has highest binding free energy (dG bind) of -54.89kcal/mol and -44.38kcal/mol respectively. Whereas native ligand has lower binding free energy compare to most active reported molecule **A** of -28.12kcal/mol and least active reported molecule **B** has weaker binding free energy of -25.57kcal/mol. Similar to the docking study, Prime MM-GBSA has been validated by using known actives and inactive and also standard drugs are incorporated in validation. This Prime MM-GBSA calculation can be used to score new ligands in order to design more potent analogues.

4.1.5. Design of New molecules

Aforementioned, Structure based drug design studies helps in prediction of the structural requirement for design of novel potent 4-(3H)-Quinazolinone antibacterial molecules. Docking studies revealed that hydrogen-bonding interaction with the substitution present at meta position of aromatic ring substituted at 3 position of quinazolinone ring might be important for activity. Docking studies also indicate that no interaction is observed for quinazolinone with SER403 residue at active site, it may be the non-covalent interactions at active site that may be responsible for anti-bacterial activity. An important aspect for inhibitor design will be to improve binding affinity by increasing the number of noncovalent interactions between inhibitor and active site.

In order to design new inhibitor, it should provide larger number of non-covalent stabilizing interactions. Alternatively, non- β -lactam compounds that bind tightly to the active site without the need for acylation with non-covalent interactions may also provide highly effective inhibitor.²⁸ The most active reported molecule **A** was considered for modification to further improve in activity. Literature indicated that direct substitution at Quinazolinone ring is not allowed.¹³ However, modification is allowed at meta position of aromatic ring substituted at 3 position of quinazolinone and at para position of aromatic ring substituted at 2 position of quinazolinone. The molecules containing amine group at meta position of aromatic ring substituted at 3 position of quinazolinone have good biological activity.^{13,29-31} Also the molecules containing electron withdrawing group at para position of aromatic ring substituted at 2 position of quinazolinone have good biological activity.¹³ Hence, modification is done at R2 position of quinazolinone by adding carbamoyl (-NHCO-) linker, followed by substitution with electron withdrawing group such as F, Cl, CN at R1 position of

Quinazolinone. New ligands mentioned in Table 3 have been designed based upon the above mentioned structure-based and ligand-based drug design studies.

4.1.6. Docking and MM-GBSA of designed molecules

All new designed molecules have been docked using same target protein 4CJN. The docking study was carried out to explore the interaction mechanism between inhibitors and the receptor. The score function of Glide, gives highest binding affinity prediction as well as molecule ranking. All molecules along with their Glide docking score have been listed in Table 3.

The binding pose of most docked ligand **8** at allosteric site shown in Figure 6. Several favorable interaction has been observed in 2D interaction image; it shows π - π interaction (green line) and π -cation (red line) of benzene ring with the residues TYR297 and LYS273 respectively. It also shows H-bond interaction (pink dotted line) between oxygen of methoxy group with the residue LYS316.

The binding pose of most docked ligand **8** at active site in 2D and 3D is shown in Figure 7. Several favorable interaction has been observed in 2D interaction image; it shows two π - π interaction (green line) between p-Cl phenyl and a substituted phenyl attached at 2-position of Quinazolinone with the residues TYR446. It also shows H-bond interaction (pink dotted line) between oxygen of amide with the residue TYR446. Similar kind of interaction is seen in 3D interaction image with some weak H-bond interaction (orange dotted line) and aromatic H-bond interaction (light blue dotted line). In 3D image H-bond is indicated by yellow dotted line, while π - π interaction is indicated by blue dotted line. Here also no interaction is observed with SER403 residue at active site.

Furthermore, all designed molecules were further subjected to Prime MM-GBSA calculations using same target protein 4CJN (Table 3). Ligand **8** has shown highest dG bind score of -52.723 and -54.628 at allosteric and active site respectively. Based on the results of docking and MM-GBSA calculation and pharmacokinetic prediction, the ligands that show good docking and dG bind score with good pharmacokinetic predictions were considered for synthesis and biological screening. The 10 best ranked designed molecules include ligand no **1**, **3**, **5**, **6**, **7**, **8**, **9**, **11**, **12** and **15** have been selected for synthesis and biological screening against microorganism.

4.2 Synthesis of Designed Ligands

All the designed compounds were synthesized by using literature reported procedures (Scheme 1) see in experimental section. N-(3-nitrophenyl)-benzamide (**1a**) and its derivatives (**1b-e**) were synthesized from literature procedure with few modifications includes using of 1.5 eq. of carboxylic acid instead of 1 eq. of carboxylic acid indicated in procedure and keep the reaction mixture for overnight.²⁰ These nitro compounds were then reduced to corresponding amine by using mixture of Fe, CaCl₂, water in Ethanol solvent to yield amine compounds (**2a-e**)²² 2-methyl-4H-benzo[d][1,3]oxazin-4-one (**3**) was synthesized by reacting anthranilic acid with triethyl ortho-acetate and reflux for 15-20min.²⁴ Compound (**2a-e**) was then reacted with compound (**3**) under acidic medium to yield compounds (**4a-e**).²⁵ Compounds (**5a-j**) were synthesized by condensation of compounds (**4a-e**) with substituted benzaldehyde under acidic medium and then reflux for 24-48 h.²⁶

Compounds (**1-5**) were characterized by elemental analysis such as IR, ¹H-NMR, ¹³C-NMR, MS (see supporting information). For example, IR-spectrum of compound (**1c**) shows an absorption bands at 3243cm⁻¹ corresponding to N-H stretch, a

band at 1661cm⁻¹ corresponding to carbonyl (C=O) of amide, and a band at 1524cm⁻¹ corresponding to characteristic C-NO₂ respectively. IR spectrum of compound (**2c**) shows a two characteristic absorption bands at 3435cm⁻¹ and 3346cm⁻¹ for NH₂ stretch, and a band at 2926cm⁻¹ corresponding to C-H stretch of alkane, while absorption band at 1651cm⁻¹ corresponding for carbonyl (C=O) of amide respectively. IR-spectrum of compounds **3** shows an absorption bands at 2970cm⁻¹ characteristic for C-H stretch of alkane, while a band at 1738cm⁻¹ corresponding to carbonyl (C=O) of lactone. IR spectrum of compound **4c** shows an absorption band at 3278cm⁻¹ corresponding to N-H stretch, and a band at 2933cm⁻¹ corresponding to C-H stretch of alkane, while at 1656cm⁻¹ corresponding to characteristic of carbonyl (C=O) amide. IR spectrum of compound **5f** shows an absorption band at 3278cm⁻¹ corresponding to N-H stretch, and a bands at 3070cm⁻¹ and 2929cm⁻¹ corresponding for C-H stretch of alkene and alkane respectively, and a band at 1656cm⁻¹ corresponding to characteristic of carbonyl (C=O) amide, Alkene C=C show a band at 1601cm⁻¹, while a band at 808cm⁻¹ for C-Cl stretch.

Proton ¹H-NMR of compound **5f** shows signal at δ : 8.34 (s, 1H, -CONH), 8.29 (d, J = 8.1 Hz, 1H, Ar-H), 7.92 (d, J = 15.4 Hz, 1H, C=C-H), 7.78 (d, J = 8Hz, 2H, Ar-H attached next to alkene), 7.70 (d, J = 7.5 Hz, 1H, Ar-H), 7.54 – 7.43 (m, J = 4Hz, 1H, Ar-H), 7.38 (d, J =8Hz, 2H, Ar-H attached next to Cl), 7.28 (dd, J = 8.4, 5.3 Hz, 2H, Ar-H), 7.21 (d, J = 8.4 Hz, 2H, Ar-H attached next to NHCOCH₂-), 6.96 (t, J = 8.5 Hz, 2H, Ar-H), 6.90 (d, J = 7.3 Hz, 1H, Ar-H), 6.84 (d, J = 8.4 Hz, 2H, Ar-H attached next to O-CH₃), 6.30 (d, J = 15.5 Hz, 1H, C=C-H), 3.75 (s, 3H, CH₃), 3.49 (s, 2H, CH₂).

Carbon ¹³C NMR of compound **5f** shows 31 carbon signal see in supporting section of which characteristic signal include: C=O of amide at 169.86, C=O of quinazolinone at 162.81, aromatic carbon attached to OCH₃ at 158.85, carbon of alkene at 139.06, aromatic carbon attached to Cl at 134.87, carbon of alkene at 114.29, carbon of OCH₃ at 55.23, carbon of CH₂ at 43.57.

The mass spectra of compounds containing Chlorine atoms (**5f** and **5h**) showed fragments corresponding to the typical chlorine isotope (³⁵Cl and ³⁷Cl). Thus, the mass spectrum of **5f** shows its M⁺ and M⁺² peaks at m/z 521.7 (66.67%) and m/z 523.7 (33.33%), respectively. (see supporting information for details)

4.3. Biological Evaluation

All synthesized compounds were evaluated for in-vitro anti-bacterial activity. The MIC values of all synthesized quinazolinone are as shown in Table 4. All of the synthesized derivative shows good range of activities against *S. aureus* (gram-positive) organism (see Figure supporting information). However, all of these compounds show weak activity against *E. coli* (gram-negative) organisms having Minimum inhibitory concentration (MIC) \geq 62.5 μ g/mL. Among all the compounds active against *S. aureus*, compound **5f** show remarkable activity with a MIC \geq 15.625 μ g/mL. Moreover, compound **5i** show moderate activity with a MIC \geq 31.25 μ g/mL. Compounds **5b**, **5d**, **5e**, **5g**, **5h** and **5j** show average activity against *S. aureus* with MIC \geq 62.5 μ g/mL. while rest of the compounds **5a** and **5c** show very weak activity with MIC \geq 125 μ g/mL. Benzamide substitution at aromatic ring of 3 position of quinazolinone with 4-fluoro styryl (compound **5a**) at 2 position of quinazolinone shows weak activity of MIC \geq 125 μ g/mL, while 4-cyano styryl (compound **5b**) substitution show little increase in activity with MIC \geq 62.5 μ g/mL. Adding methyl at 2-position of benzamide shows no improvement in activity with MIC \geq 125 μ g/mL and MIC \geq 62.5 μ g/mL for 4-fluoro styryl (compound **5c**) and 4-

ciano styryl (compound **5d**) substitution respectively. Adding two methoxy group at 3 and 4 position of benzamide substituted at aromatic ring of 3 position of quinazolinone show little improvement in activity with both 4-fluoro styryl (compound **5g**) and 4-Chloro styryl (compound **5h**) substitution at 2 position of quinazolinone with an MIC \geq 62.5 μ g/mL.

However, adding methylene linker in between amide and 4-methoxy phenyl substituted at aromatic ring of 3 position of quinazolinone shows no improvement in activity with 4-fluoro styryl (compound **5e**) substitution at 2 position of quinazolinone with MIC \geq 62.5 μ g/mL, while 4-Chloro styryl (compound **5f**) substitution show good activity with MIC \geq 15.625 μ g/mL.

Although replacing benzamide with thiophene-2-carboxamide shows improvement in activity, 4-fluoro styryl (compound **5i**) substitution at 2 position of quinazolinone show moderate activity with MIC \geq 31.25 μ g/mL, while 4-cyano styryl (compound **5j**) substitution at 2 position of quinazolinone shows weak activity with MIC \geq 62.5 μ g/mL.

Moreover, all synthesized compounds were also tested against Methicillin resistant *staphylococcus aureus* (MRSA) (ATCC). Compound **5f** and compound **5i** shows good activity with MIC \geq 31.25 μ g/mL, while rest of the compounds **5a**, **5b**, **5c**, **5d**, **5e**, **5g**, **5h**, and **5j** shows weak activity with MIC \geq 62.5 μ g/mL.

Table 1. Summary of Docking and MM-GBSA score at allosteric and active site. Docking score MM-GBSA

	Docking score		MM-GBSA	
	Allosteric site	Active site	Allosteric site	Active site
Most active reported molecule A	-4.579	-4.834	-47.41	-43.43
Least active reported molecule B	-1.199	-1.603	-22.42	-25.57
Native ligand	-3.581	-4.795	-38.35	-28.12
Ceftaroline	-5.558	-5.334	-50.36	-54.89
Ceftobiprole	-4.64	-5.291	-42.13	-44.38

Table 2. Summary of QikProp studies.

	Most active reported molecule A	Least active reported molecule B	Ceftaroline fosamil	Ceftobiprole medocaril
#stars	0	1	2	2
LogP o/w	2.509	4.261	1.667	2.466
QPPCaco	853.02	464	545	690
% Human oral absorption	76.19	100	100	95
Rule of five ^[a]	0	0	2	2

^[a]value indicate violation in Lipinski's rule of five.

Where,

#stars: A large number of stars suggest that a molecule is less drug-like than molecules with few stars.

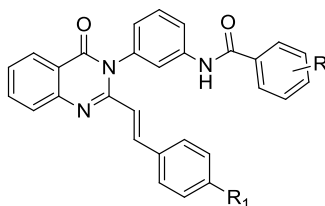
Log P: Predicted octanol/water partition coefficient.

QPPCaco: Predicted apparent Caco-2 cell permeability in nm/sec. Caco-2 cells is a model for the gut-blood barrier. QikProp predictions are for non-active transport.

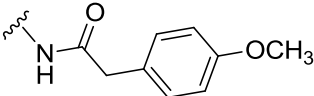
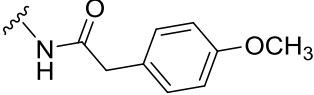
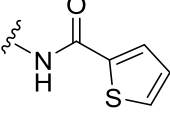
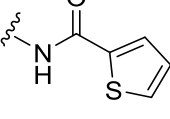
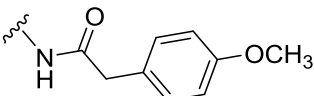
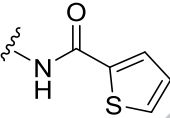
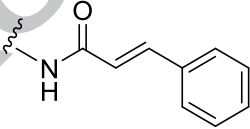
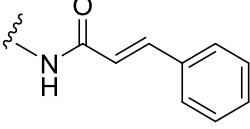
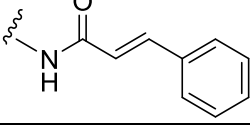
Percent Human Oral Absorption: Predicted human oral absorption on 0 to 100% scale.

^aRule of Five: Number of violations of Lipinski's rule of five. The rules are: mol-MW < 500, logP o/w \leq 5, donorHB \leq 5, acceptHB \leq 10. Compounds that satisfy these rules are considered as druglike molecule.

Table 3. Designed molecules

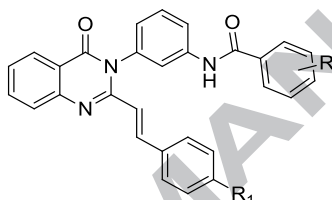


Ligand no.	R	R ₁	Docking score		MM-GBSA (dG bind)		Rule of five ^[a]	LogP
			Allosteric site	Active site	Allosteric site	Active site		
1	H	F	-3.538	-3.672	-49.752	-41.158	1	5.174
2	H	Cl	-3.594	-2.849	-54.437	-35.76	1	5.146
3	2-CH ₃	F	-3.929	-3.684	-44.573	-43.64	1	5.396

4	2-CH ₃	Cl	-3.584	-3.183	-54.646	-32.095	2	5.612
5	3,4-DiOCH ₃	F	-4.413	-3.886	-51.445	-40.979	2	4.792
6	3,4-DiOCH ₃	Cl	-4.066	-3.686	-59.734	-43.319	2	4.649
7		F	-3.964	-3.865	-50.221	-51.977	1	4.916
8		Cl	-4.674	-4.327	-52.723	-54.628	1	4.758
9		F	-3.618	-3.632	-52.99	-38.124	1	5.012
10		Cl	-3.618	-2.992	-51.539	-36.021	0	4.924
11	H	CN	-4.187	-3.464	-47.929	-42.367	1	5.124
12	2-CH ₃	CN	-4.261	-3.796	-50.275	-46.09	1	4.6
13	3,4-DiOCH ₃	CN	-3.979	-3.898	-55.977	-24.979	1	4.764
14		CN	-3.834	-4.086	-51.64	-39.512	0	4.747
15		CN	-3.627	-3.655	-53.981	-41.733	1	5.862
16	2-OH	F	-3.196	-3.067	-30.58	-24.168	1	6.118
17	2-OH	Cl	-3.149	-3.141	-33.598	-35.739	0	4.843
18	2-OH	CN	-3.674	-3.737	-39.906	-44.249	1	6.584
19		F	-4.02	-3.138	-54.948	-32.061	2	6.785
20		Cl	-3.624	-2.645	-55.573	-37.253	1	5.507
21		CN	-4.157	-2.834	-50.637	-37.222	0	4.317

22		F	-4.4	-3.546	-49.873	-31.571	0	4.564
23		Cl	-4.043	-3.043	-47.381	-21.429	0	3.217
24		CN	-4.579	-4.258	-50.035	-40.381	1	6.465
25	4-Cl	F	-3.727	-3.553	-47.751	-32.372	2	6.694
26	4-Cl	CN	-3.728	-4.187	-59.819	-36.475	1	6.174

Table 4 Antimicrobial activities of test compounds



Molecule no	R	R ₁	Bacteria MIC (µg/mL)		
			Gram-negative	Gram-positive	
			<i>Escherichia coli</i>	<i>Staphylococcus aureus</i>	Methicillin- Resistant <i>Staphylococcus aureus</i> (MRSA)
5a	H	F	62.5	125	62.5
5b	H	CN	62.5	62.5	62.5
5c	2-CH ₃	F	62.5	125	62.5
5d	2-CH ₃	CN	62.5	62.5	62.5
5e		F	62.5	62.5	62.5
5f		Cl	62.5	15.625	31.25
5g	3,4-DiOCH ₃	F	62.5	62.5	62.5
5h	3,4-DiOCH ₃	Cl	62.5	62.5	62.5
5i		F	62.5	31.25	31.25
5j		CN	62.5	62.5	62.5
Standard drugs	Streptomycin		7.8	7.8	-
	Kanamycin		7.8	7.8	-
	Linezolid		-	-	7.8

5. Conclusions

The present research has been carried out to develop new molecules by structure based drug design. Docking studies has been carried out to explore the interaction between ligands and the receptor. Docking study explained the importance of hydrogen bonding interaction with the substitution present at meta position of aromatic ring substituted at 3 position of quinazolinone ring for activity. The most active reported molecule **A** displays a H-bond interaction between amine of mesyl group with residues of target protein and therefore, the position has been selected for modification. Furthermore, all designed molecules were further subjected to Prime MM-GBSA calculations to determine binding free energy.

Based on the result of molecular modelling studies 26 new ligands have been designed which were ranked as good ligand by using docking interaction study and prime MM-GBSA calculation and then in-silico pharmacokinetic properties of designed molecules were determines by ADME prediction software, Qikprop. These predictions help to identify potential drug like molecule. Out of 26 designed ligands, 10 best ranked ligands have been selected depend upon their docking, MM-GBSA, and ADME prediction which then considered for synthesis and followed by biological screening of anti-bacterial activity.

These 10 designed molecules have been synthesized by appropriate conventional synthetic route see in experiment section. After synthesis, these molecules were screened for biological activity against three bacterial strains namely *E. coli*, *S. aureus*, Methicillin resistant *Staphylococcus aureus*. All of these ligands show weak activity against gram negative organism *E. coli*, while shows moderate to good activity against gram positive organism *S. aureus* of which ligand **5f** has shown most potent activity with MIC \geq 15.625 μ g/mL against *S. aureus*. These ligands were also tested against resistant strain of *S. aureus* i.e. MRSA, the ligand **5f** and **5i** shows good activity with MIC \geq 31.25 μ g/mL. Thus, the molecular modelling studies assist in design of new analogues that would further enhance the biological activity.

In present study, Structure based drug design has been performed for Quinazolinone molecule with Penicillin binding protein 2a (PBP2a). This study will help to understand how non β -lactam able to inhibit cell wall inhibition similar to β -lactam. This studies further help to identify the potential lead molecules by virtual screening and optimization of the lead molecules.

Acknowledgments

SIQ and HKC thank to Merck India for providing financial facility.

References and notes

- Boucher, H.W.; Talbot, G.H.; Bradley, J.S.; Edwards, J.E.; Gilbert, D.; Rice, L.B.; Scheld, M.; Spellberg, B.; Bartlett, J. *Clin. Infect. Dis.* **2009**, *48*, 1-12.
- Staph infection can kill, *Cent. Dis. Control Prev.* **2019**. <https://www.cdc.gov/vitalsigns/staph/pdf/vs-0305-staph-infections-H.pdf> (accessed April 25, 2019).
- Rice, L.B. *J. Infect. Dis.* **2008**, *197*, 1079-1081.
- Pitout, J.D.; Sanders, C.C.; Sanders, W.E. *Am. J. Med.* **1997**, *103* (1997) 51-59.
- Hartman, B.J.; Tomasz, A.; *Bacteriol.* **1984**, *158*, 513-516.
- Biek, D.; Critchley, I.A.; Riccobene, T.A.; Thye, D.A.; *J. Antimicrob. Chemother.* **2010**, *65*, 9-16. doi:10.1093/jac/dkq251.
- Fuda, C.; Heseck, D.; Lee, M.; Morio, K.I.; Nowak, T.; Mobashery, S. *J. Am. Chem. Soc.* **2005**, *127*, 2056-2057.
- Otero, L.H.; Rojas-Altuve, A.; Llarrull, L.I.; Carrasco-López, C.; Kumarasiri, M.; Lastochkin, E.; Fishovitz, J.; Dawley, M.; Heseck, D.; Lee, M.; Johnson, J.W.; Fisher, J.F.; Chang, M.; Mobashery, S.; Hermoso, J.A. *Proc. Natl. Acad. Sci. U. S. A.* **2013**, *110*, 16808-16813.
- Fishovitz, J.; Rojas-Altuve, A.; Otero, L.H.; Dawley, M.; Carrasco-Lopez, C.; Chang, M.; Hermoso, J.A.; Mobashery, S.; *J. Am. Chem. Soc.* **2014**, *136*, 9814-9817.
- Sahm, D.F.; Deane, J.; Bien, P.A.; Locke, J.B.; Zuill, D.E.; Shaw, K.J.; Bartizal, K.F. *Microbiol. Infect. Dis.* **2015**, *81*, 112-118.
- Morales, G.; Picazo, J.J.; Baos, E.; Candel, F.J.; Arribi, A.; Peláez, B.; Andrade, R.; de la Torre, M.-A.; Fereres, J.; Sánchez-García, M. *Clin. Infect. Dis.* **2010**, *50*, 821-825.
- R. Botley, M. Kumarasiri, Z. Peng, L.H. Otero, W. Song, M.A. Suckow, V.A. Schroeder, W.R. Wolter, E. Lastochkin, N.T. Antunes, H. Pi, S. Vakulenko, J.A. Hermoso, M. Chang, S. Mobashery, *J. Am. Chem. Soc.* **2015**, *137*, 1738-1741.
- Bouley, R.; Ding, D.; Peng, Z.; Bastian, M.; Lastochkin, E.; Song, W.; Suckow, M.A.; Schroeder, V.A.; Wolter, W.R.; Mobashery, S.; Chang, M. *J. Med. Chem.* **2016**, *59*, 5011-5021.
- Glide 6.3, Schrödinger, LLC, New York, NY, 2016
- Rani, N.; Saravanan, V.; L.P.T. V. Arunachalam, A. *J. Biomol. Struct. Dyn.* **2015**, *1102*, 1-35.
- QikProp 4.3, Schrödinger, LLC, New York, NY, 2016.
- Balaji, B.; Hariharan, S.; Shah, D.B.; Ramanathan, M. *Eur. J. Med. Chem.* **2014**, *86*, 469-480.
- Prime, Schrödinger, LLC, New York, NY, 2016
- Riss, T.; Moravec, R. *Promega Notes.* **2003**, 10-13.
- Leggio, A.; Belsito, E.L.; De Luca, G.; Di Gioia, M.L.; Leotta, V. Romio, E.; Siciliano, C.; Liguori, A. *RSC Adv.* **2016**, *6*, 34468-34475.
- Wang, J.; Yin, X.; Wu, J.; Wu, D.; Pan, Y. *Tetrahedron.* **2013**, *69*, 10463-10469.
- Chandrappa, S.; Vinaya, K.; Ramakrishnappa, T.; Rangappa, K.S. *Synlett.* **2010**, *14*, 3019-3022.
- Al-Nadaf, A.; Sheikha, G.A.; Taha, M.O. *Bioorg. Med. Chem.* **2010**, *18*, 3088-3115.
- Khajavi, M.S.; Montazari, N.; Hosseini, S.S.S. *J. Chem. Res.* **1997**, 286-287.
- Mosley, C.A.; Acker, T.M.; Hansen, K.B.; Mullasseril, P.; Andersen, K.T.; Le, P.; Vellano, K.M.; Bräuner-Osborne, H.; Liotta, D.C.; Traynelis, S.F. *J. Med. Chem.* **2010**, *53*, 5476-5490.
- Raffa, D.; Edler, M.C.; Daidone, G.; Maggio, B.; Merickech, M.; Plescia, S.; Schillaci, D.; Bai, R.; Hamel, E. *Eur. J. Med. Chem.* **2004**, *39*, 299-304.
- Silva IC, Ferreira H. *Bio-protocol.* 2013, 3, 1-4.
- Lim, D.; Strynadka, N.C.J. *Nat. Struct. Biol.* **2002**, *9*, 870-876.
- Zayed, M. F.; Hassan, M. H. *Saudi Pharm. J.* **2014**, *22*, 157-162.
- H.U. S, Reddy, G.K. *In Vitro.* **2012**, *1*, 690-696.
- Saravanan, G.; Alagarsamy, V.; Prakash, C.R. *J. Saudi Chem. Soc.* **2011**, *19*, 3-11.

Supplementary Material

Supplementary information file is provided

[Click here to remove instruction text...](#)

Highlights:

- Resistance in methicillin-resistant *Staphylococcus aureus* (MRSA) due to acquisition of additional PBP2a.
- CADD explore the structural features of Quinazolinone as anti-MRSA agents.
- New molecules have been designed by using docking using PBP2a target.
- Most compound were active against *S. aureus*, While few show activity against MRSA.
- The compound **5f** shows good activity against MRSA.